

# Switchable Wideband Terahertz Absorber Based on Refractory and Vanadium Dioxide Metamaterials

Jinglei Wang, Yu Yao, Xiaoshan Liu<sup>✉</sup>, Guiqiang Liu, *Member, IEEE*, and Zhengqi Liu<sup>✉</sup>

**Abstract**—Achieving actively tunable metamaterial absorption is a significant development direction. Phase-transition materials have attracted growing interest for the use in nanophotonics owing to their flexibility. In this work, we firstly demonstrate a wideband terahertz refractory absorber that achieves more than 90% absorptance in the range of 1.71–3.31 THz. The metal composing the structure is refractory metal, which could function in high-temperature conditions and complex electromagnetic environment. Then, we incorporate phase-change material vanadium dioxide ( $\text{VO}_2$ ) film to this refractory absorber, realizing high reflection of more than 93% in the metallic state, while the wideband perfect absorption peak over 98% is obtained in the insulating state. Calculated results show that metamaterial absorber obtains switchable functions. Furthermore, the tunable absorber has polarization-insensitive behavior. So, our designed absorber with dynamic tunable characteristics provides flexibility to adjust the absorption performance and has significant value in application. The proposed architecture offers a novel method for creating dynamic and multi-functional photonic devices in phase-change materials.

**Index Terms**—Metasurface, refractory, terahertz, tunable, vanadium dioxide ( $\text{VO}_2$ ).

## I. INTRODUCTION

METAMATERIALS, artificially made of periodic structures possessing many exotic properties not seen in nature materials, such as negative permittivity and negative permeability [1], [2], [3], zero permittivity, zero permeability [4], [5], and strong anisotropic permittivity or permeability tensor [6], [7]. The control of the electromagnetic structure is accomplished by altering the unit structure, cycle, length, material, and other characteristics. Metamaterial absorbers have drawn a lot of attentions due to the novel optical properties, such as reflection, absorption, scattering and so on [8], [9]. A typical structure like the shape of sandwich is widely designed in the metamaterial absorber due to the generation of F-P cavity resonance. In 2008, a metamaterial absorber based on the metal-insulator-metal (MIM) structure was designed by Landy et al. The absorber achieves absorptance of 88% at 11.5 GHz, and this pioneering study opens a new

TABLE I  
MELTING POINTS OF MATERIAL COMMONLY USED IN ABSORBER

material	Melting points/°C	material	Melting points/°C
W	3422	$\text{ZrB}_2$	3060
Mo	2623	TiN	2930
Cr	1875	SiC	2830
Ti	1668	$\text{TiO}_2$	1840
Au	1063	$\text{Al}_2\text{O}_3$	1778
Ag	961	$\text{SiO}_2$	1600

way for further optical absorption investigations in metamaterial absorbers [10]. Many researchers have designed the structure of a practical value, such as the solar photovoltaic (Solar thermal photovoltaics STPVs) [11], photoelectric detector [12], and other electronic and optical sensor device [13].

It is well known that precious metal has plasmon resonance and optical coupling behavior and is widely used to make solar absorber [14], [15]. However, precious metals have low melting points and high prices, which limit their wide use for making absorbers. Refractory metal have significant value in application due to their high melting points and good stability [16], [17]. Titanium (Ti) has a melting point of 1660 °C, so it can be widely used in high-temperature condition as a refractory metal. Then the compounds of Ti are also refractory materials. They are available in larger quantities and at lower costs compared to precious metal. Common materials in absorbers are listed in the Table I. Deng et al. designed a wideband refractory structure composed of Cr rings and reflective Cr mirror, which achieved high absorption of over 80% in the infrared range. In 2018, Chen et al. designed a broadband absorber that have a high absorption of 89% and 83.26% at the temperatures of 800 K and 1000 K [18]. Therefore, it is of great significance to use refractory materials for metal-based resonant systems.

The properties of previous metamaterials are not easily changed once their structure is determined. According to the former study, using tunable materials is an excellent method to overcome the limitation, such as liquid crystal [19],  $\text{Ge}_2\text{Sb}_2\text{Te}_5$ (GST) [20],  $\text{VO}_2$  [37], and graphene [22], reconfigurable metal [23]. Phase-change materials have drawn a lot of attention in the realm of active photonics because of their excellent electrical and optical capabilities [24], [25], [26], [27].

Manuscript received 27 November 2022; revised 28 December 2022; accepted 3 January 2023. Date of publication 6 January 2023; date of current version 13 January 2023. This work was supported in part by the National Natural Science Foundation of China (NSFC) under Grants 62065007, 11804134, and 62275112, and in part by the Natural Science Foundation of Jiangxi Province under Grant JXSQ2019201058. (*Corresponding author: Xiaoshan Liu; Zhengqi Liu.*)

The authors are with the College of Physics and Communication Electronics, Jiangxi Normal University, Nanchang, Jiangxi 330022, China (e-mail: 202040100572@jxnu.edu.cn; 1936810251@qq.com; xsliu@jxnu.edu.cn; liugq@jxnu.edu.cn; zliu@jxnu.edu.cn).

Digital Object Identifier 10.1109/JPHOT.2023.3234535

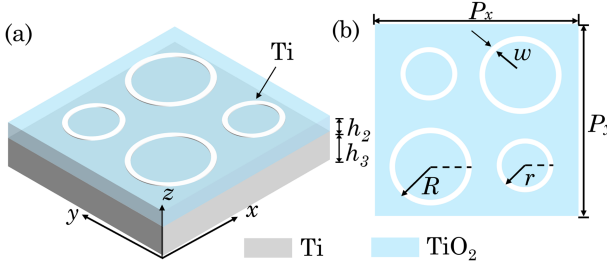


Fig. 1. Schematic of the designed terahertz refractory metamaterial absorber consisting of Ti substrate, TiO<sub>2</sub> layers and four Ti rings. (a) one unit structure of the absorber, (b) the top view of the absorber.

VO<sub>2</sub> is the typical example of phase-change materials [28], [29], [30]. Its dielectric permittivity will change remarkably in the process of phase transition. It can change from the insulator state to metallic state when the temperature is above 68 °C [31], so its structural phase transition will also change and has a large strain [32]. Different applications of VO<sub>2</sub> have been explored a lot, such as modulator [33], temperature sensor, [34] rewritable device [35] and optical switch [36]. To date, there are little research focused on the integration of switchable and refractory functionalities in the terahertz (THz) range. For example, Ding et al. proposed a switchable absorber based VO<sub>2</sub> which can switch the function from broadband absorption with bandwidth of 0.67 THz to reflection [11]. Ren et al. theoretically designed an absorber based on the phase-change material of VO<sub>2</sub>, which can realize circular dichroism to asymmetric transmission effect [37]. Song et al. proposed a multilayer metamaterial based VO<sub>2</sub> which could change the absorption bandwidth greatly [38]. Then, utilizing the phase transition of VO<sub>2</sub>, they designed a broadband absorber with a bi-function and polarization converter based on a switchable metasurface [39].

In this work, a sandwich structure absorber composed of refractory materials is designed. The absorber obtains perfect multi-band absorption due to the excitation of dipole resonance. The intrinsic mechanism is explored by analyzing the electric field distribution and absorption spectra with changing the geometrical parameters. Then, the introduce of VO<sub>2</sub> achieves a switchable function of the refractory absorber with the intermediate structure of VO<sub>2</sub>. It realizes wideband perfect absorption obviously in the range of 2.23–3.18 THz when VO<sub>2</sub> in the insulating state, while realizing high reflection more than 93% when VO<sub>2</sub> in the metallic state. To better analyze the performance, the influence of polarization angle and thickness of VO<sub>2</sub> is investigated. It is can be concluded that the introduction of VO<sub>2</sub> plays the essential role in tunable absorbers.

## II. DESIGN AND METHOD

Fig. 1 shows that the terahertz refractory wideband absorber consisting of three layers, which are resonant unit, titanium dioxide (TiO<sub>2</sub>) layer, and titanium (Ti) substrate. Multiple resonant modes are excited by two kinds of sizes Ti ring resonant units to broaden the absorption bandwidth. The period  $P_x = P_y = 79 \mu\text{m}$ , the outer radius of the large Ti rings  $R = 16 \mu\text{m}$ , the outer radius of the small Ti rings  $r = 11 \mu\text{m}$ , the width of Ti ring  $w = 1 \mu\text{m}$ ,

the thickness of resonant units  $h_1 = 0.5 \mu\text{m}$ , the thickness of TiO<sub>2</sub> layer  $h_2 = 19 \mu\text{m}$  and the Ti substrate  $h_3 = 35 \mu\text{m}$ . The material selection of Ti and TiO<sub>2</sub> used comes from palik [40].

Then, we add the phase-change material VO<sub>2</sub> film to this structure. Keeping the above structure unchanged, the increased VO<sub>2</sub> thickness  $h_4 = 0.9 \mu\text{m}$ . The Drude model [41] can illustrate the relevant dielectric constant of the VO<sub>2</sub> in different state,

$$\varepsilon(\omega) = \varepsilon_{\infty} - \frac{\omega_p^2(\sigma)}{\omega^2 + i\gamma\omega} \quad (1)$$

The high frequency dielectric permittivity  $\varepsilon_{\infty} = 12$ .  $\omega p(\sigma)$  is the plasma frequency that is dependent on conductivity,  $\gamma$  is the collision frequency.  $\omega p^2(\sigma)$  and  $\omega$  are proportional to free carrier density. The plasma frequency  $\omega p(\sigma)$  is described as

$$\omega p(\sigma)^2 = \frac{\sigma}{\sigma_0} \omega p(\sigma_0)^2 \quad (2)$$

$\sigma_0 = 3 \times 10^3 \Omega^{-1}\text{cm}^{-1}$ ,  $\omega p(\sigma_0) = 1.40 \times 10^{15} \text{ rad/s}$ , and  $\gamma = 5.75 \times 10^{13} \text{ rad/s}$  which is independent of  $\sigma$  [21]. we simulate metal phase of VO<sub>2</sub> with the conductivity of  $\sigma = 2 \times 10^5 \text{ S/m}$  and realize insulator phase with the conductivity of  $\sigma = 0 \text{ S/m}$ . According to the characteristics of VO<sub>2</sub>, the incident electromagnetic wave is reflected when it is in the metallic state. It is equivalent to the dielectric layer when it is in the insulating state, the upper metal ring resonance unit, the dielectric layer TiO<sub>2</sub> and the underlying refractory Ti form a MIM resonator to absorb the electromagnetic waves.

## III. RESULTS AND DISCUSSIONS

### A. Absorption Performance of Refractory Metamaterial Wideband Absorber

The absorption response of the designed absorber was calculated by the finite-difference time-domain (FDTD) method. We simulate one period of the structure in calculation. The periodic boundary condition was set in  $X$  and  $Y$  directions, perfectly matched layer (PML) was set in  $Z$  direction. In the simulation, the absorptance ( $A$ ) can be expressed by the expression  $A = 1 - R - T$  [42], [43], [44], [45], the indices  $R$  and  $T$  signify the reflection and transmittance. The thickness of Ti substrate  $h_3 = 35 \mu\text{m}$ , so transmission is almost negligible. Therefore, we can simply compute the absorptance ( $A$ ) from the equation  $A = 1 - R$ .

Fig. 2 illustrates the spectrum performance of the wideband refractory absorber in the range of 0.8–4 THz. It clearly suggests that four different absorption peaks at 0.93 THz, 1.95 THz, 2.56 THz and 3.10 THz, the designed absorber can absorb more than 90% in the range of 1.71–3.31 THz with absorption bandwidth of 1.60 THz and a relative absorption bandwidth  $Bw = 63.75\%$ . Therefore, we can conclude that the refractory metamaterial absorber has an excellent effect with high broadband absorption spectrum. To further deeply understand the intrinsic mechanism of the multi-band near-perfect absorption phenomenon, we simulated the electric field distribution of this refractory absorber structure at the peaks  $f_1, f_2, f_3$ , and  $f_4$ . As shown in Fig. 3(a)–(d), it is observed that strong electric fields existed at the ring resonators. The corresponding surface current distributions on

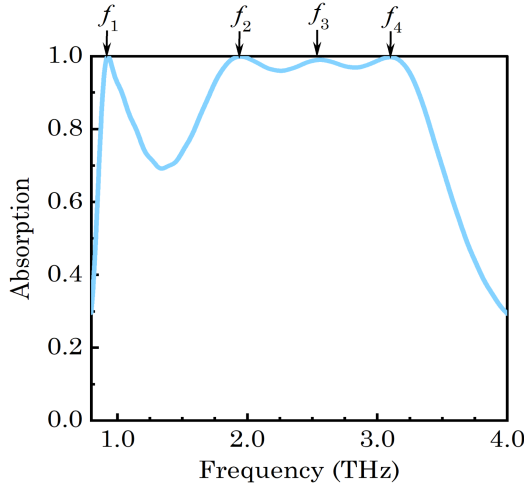


Fig. 2. The absorption spectra of the absorber based refractory metamaterial, the resonance frequency  $f_1 = 0.93$  THz,  $f_2 = 1.95$  THz,  $f_3 = 2.56$  THz,  $f_4 = 3.10$  THz.

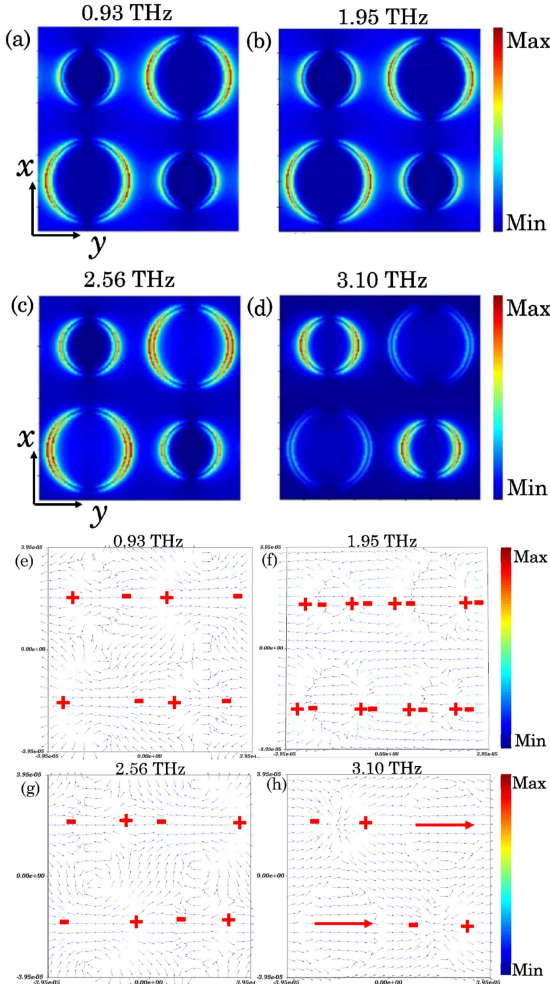


Fig. 3. The electric fields (a)–(d) and current (e)–(h) distributions in the  $Z$  direction at the four perfect absorption frequency points of 0.93 THz, 1.95 THz, 2.56 THz, 3.10 THz.

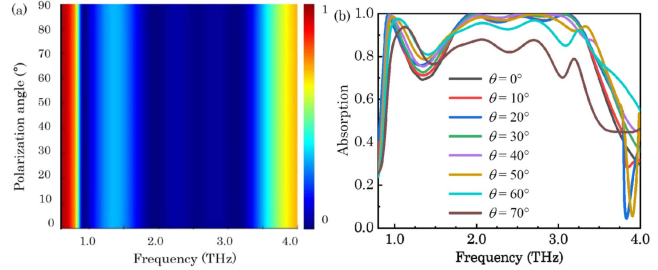


Fig. 4. (a) Reflection at different polarization angles. (b) Absorption curve with incident angle within  $70^\circ$ .

the top rings are shown in Fig. 3(e)–(h). In Fig. 3(e), (g), it is seen that the surface currents on the two sides of the rings are opposite to each other, resulting in a strong electric dipole [46]. In Fig. 3(f), each side of the rings generates the electric dipole. Fig. 3(h) suggests that the electric dipole exists on the small rings, and current flows from left to right of the large rings, which inspires surface plasmon (LSP). So, electric dipole resonance makes the main contribution to the absorption peak at frequency  $f_1$ ,  $f_2$ , and  $f_3$ , and the dipole resonance and LSP contributes to the strong absorption peak at frequency  $f_4$ . There are no opposite current distributions on the bottom Ti substrate and top Ti rings, so there has no magnetic dipole [47]. Thereby, the introduced different metal rings can strongly enhance the ED resonance realizing the near perfect absorption peaks.

The performance of changing polarization angles was also investigated [48]. In Fig. 4(a), the reflection remains unchanged with the polarization increases from  $0^\circ$  to  $90^\circ$ , the plot clearly indicates that the absorption is completely independent of polarization, which can be ascribed to the symmetry of this designed structure, so we can conclude that this structure has great polarization-insensitive properties. In practice, the incident angle of electromagnetic wave has different incident directions, so the polarization-independence can provide crucial value for the absorber. As can be seen in Fig. 4(b), as the incident angle varies from  $0^\circ$  to  $70^\circ$ , the absorptance remains 90% in the narrow-band range, and the absorptance does not change obviously and maintains absorptance of over 90% in the range of  $0^\circ$  to  $40^\circ$  in the broadband range. When the incidence angles reached  $70^\circ$ , the absorption also remains above 70%, which caused by the increasing of incidence angle, and the electric field intensity decreases, so the ED resonance absorption in the four metal rings will weaken.

It is significant to investigate the influence of changing geometric parameters of this designed structure. In the Fig. 5, we plot the absorption curves of changing ring's radius  $R$  and  $r$ , the width  $w$  and the  $\text{TiO}_2$  layer's thickness  $h_2$  without changing other parameters. In Fig. 5(a), the absorption peak shows a red-shift as  $R$  increasing. Specifically, since the absorption at 3.10 THz is provided by the small rings, changing the radius of large rings will not affect the electric field at the frequency point, but the change of large rings leads to frequency shift and absorption changes in other three frequency points. In Fig. 5(b), when the

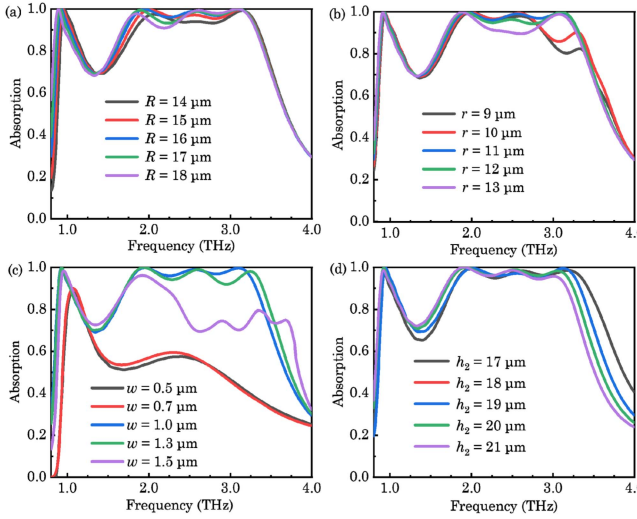


Fig. 5. (a)–(d) The measured absorptance spectra of changing the large ring radius “ $R$ ”, small ring radius “ $r$ ”, ring width “ $w$ ”, and  $\text{TiO}_2$  thickness “ $h_2$ ”, the other geometric parameters remain unchanged.

small ring radius  $r$  changes from 9  $\mu\text{m}$  to 13  $\mu\text{m}$ , the curve is redshifted, affecting the absorption at 2.56 THz and 3.10 THz, the absorptance reaches a maximum when  $r = 11 \mu\text{m}$ , and the absorption at the other two points hardly changes. In Fig. 5(c), when the ring width is changed, the absorption changes greatly, and reach high absorptance at  $w = 1 \mu\text{m}$ . In Fig. 5(d), it is found that the change of the thickness of  $\text{TiO}_2$  make the curve redshift, since the absorption is mainly ascribed to the function of dipole resonance, the change of the  $\text{TiO}_2$  thickness will affect the coupling degree, and decrease the absorptance of this system.

### B. Absorption Performance of Tunable Wideband Absorber Based $\text{VO}_2$

As for the  $\text{VO}_2$ , there is the relationship between temperature and conductivity [49]. the conductivity changed greatly with the increase of temperature, so it is feasible for practical implementation for  $\text{VO}_2$  based switchable design. In Fig. 6(a), we add a  $\text{VO}_2$  film to the refractory metamaterial absorber. The four layers structure of vanadium dioxide and refractory materials active tunable absorber was established. Keeping the above structure unchanged, the thickness of  $\text{VO}_2$  is  $h_4 = 0.9 \mu\text{m}$ .  $\text{VO}_2$  possesses the feature that the lattice structure can be changed by heating and light. According to the characteristics of  $\text{VO}_2$ , in Fig. 6(b), when  $\text{VO}_2$  is in the insulate state, the upper metal ring resonance unit, the dielectric layer  $\text{TiO}_2$  and the underlying refractory  $\text{Ti}$  form a MIM resonator to absorb the electromagnetic waves. When the temperature increases to 68  $^\circ\text{C}$  by heating or electrical excitation,  $\text{VO}_2$  is in the metal state, the high reflection of incident electromagnetic wave is realized. In Fig. 6(b), when  $\text{VO}_2$  is in insulating state (blue line), we can obviously see the absorption peak of 98% at 1.02 THz. In the range of 2.23–3.18 THz, the absorptance reaches more than 90% and the bandwidth ratio is 35.12%. When  $\text{VO}_2$  is in metal state (red line), the absorptance is mutated to below 7%, achieving the great effectiveness of high reflection. Therefore, the absorber

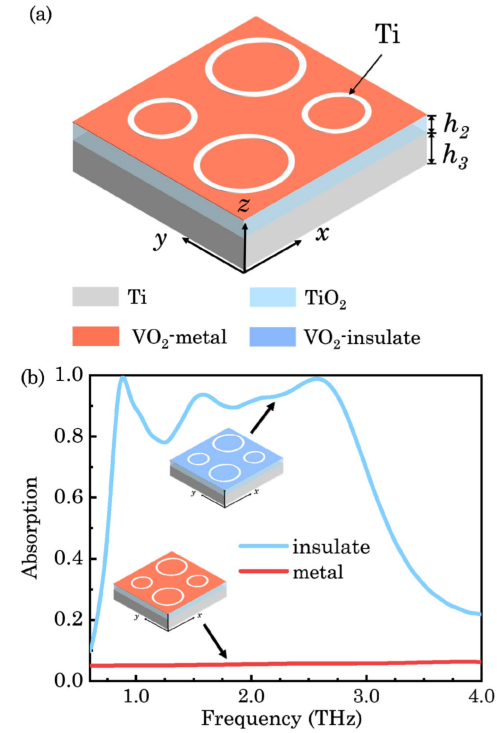


Fig. 6. (a) Schematic diagram of the  $\text{VO}_2$  absorber. (b) Absorption curve under metal state (red) and insulating state (blue).

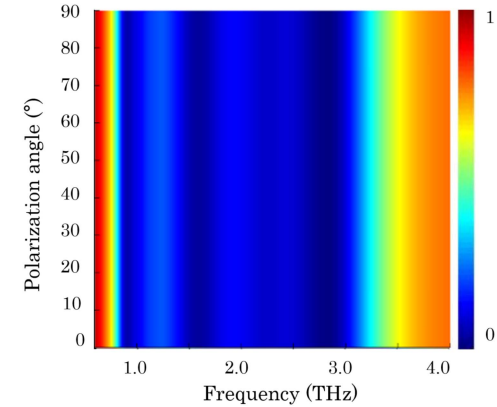


Fig. 7. Reflection at different polarization angles.

realizes the “switch” function by incorporating the phase-change materials  $\text{VO}_2$  into the refractory wideband absorber, its function changes from a simple broadband absorber to a tunable absorber and it still remains a wide range of absorptance.

In Fig. 7, when  $\text{VO}_2$  is in insulating state, the absorptance evolution spectrum of the tunable absorber by changing the polarization angle is showed. When the polarization angle increases from 0° to 90°, the absorptance spectrum of the structures is unchanged, which clearly displays the independent of the polarization angle, and has the polarization-insensitive property. This is of great significance for practical applications.

Furthermore, to better comprehend the performance of the actively tunable wideband refractory absorber, we analyzed the influence of thickness of  $\text{VO}_2$  ( $h_4$ ). Fig. 8(a) shows the

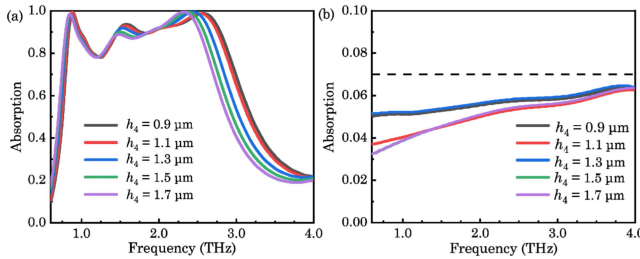


Fig. 8. The effect of varying  $\text{VO}_2$  thickness on absorption in metal (a) and insulation (b), respectively.

relationship between absorptance and the thickness of  $\text{VO}_2(h_4)$ , when  $h_4$  increases from 0.9  $\mu\text{m}$  to 1.7  $\mu\text{m}$ , this absorptance curve increases and has red-shifts, which is due to the increasing of the  $\text{VO}_2$  thickness leads to the increasing of the media layer thickness. Then, the media layer thickness will affect the dipole resonance, so that the curve will undergo an expected redshift. The impedance of this structure exactly matches to the impedance of free space, and then minimize the reflection at a specific frequency. In Fig. 8(b), there was a slight change in the absorption after changing the  $\text{VO}_2$  thickness when  $\text{VO}_2$  is in metallic state, and due to the reflection of the electromagnetic wave on the  $\text{VO}_2$  film. In all, when the thickness of  $\text{VO}_2$  is 0.9  $\mu\text{m}$ , the absorber achieved wideband high absorption over 98% and high reflection below 7% in the insulating and metallic state, respectively. The switchable wideband terahertz absorbers can be widely used in the many potential switchable and photonics devices.

#### IV. CONCLUSION

In summary, we firstly proposed a switchable terahertz absorber based on refractory Ti metal achieved high absorptance over 90% in the range of 1.71–3.31 THz. We stimulate the electric field and changed geometric parameters of the system to investigate the intrinsic mechanism. More than that, titanium and titanium dioxide are fire-resistant, they can work at high temperatures and have practical applications. Secondly, the phase-change material  $\text{VO}_2$  was incorporated to this absorber, a switchable terahertz metamaterial absorber was designed by adjusting work temperature, realizing “switch” from perfect absorption peak over 98% in the insulating state to high reflection ( $A < 7\%$ ) in the metallic state. Therefore, the use of  $\text{VO}_2$  can realize outstanding tunable function of the absorptance of electromagnetic waves. Moreover, the absorber has polarization-insensitive characteristic. Therefore, the terahertz absorber can flexibly control the absorption performance with dynamic tuning characteristics, and provides an excellent method for the advancement of optical switch, photonics devices, modulation, and so on.

#### REFERENCES

- [1] N. Engheta and R. W. Ziolkowski, “A positive future for double-negative metamaterials,” *IEEE Trans. Microw. Theory Techn.*, vol. 53, no. 4, pp. 1535–1556, Apr. 2005.
- [2] W. Withayachumnankul and D. Abbott, “Metamaterials in the terahertz regime,” *IEEE Photon. J.*, vol. 1, no. 2, pp. 99–118, Aug. 2009.
- [3] N. Yu, F. Aieta, P. Genevet, M. A. Kats, Z. Gaburro, and F. Capasso, “A broadband, background-free quarter-wave plate based on plasmonic metasurfaces,” *Nano Lett.*, vol. 12, no. 12, pp. 6328–6333, Dec. 2012.
- [4] X. Huang, Y. Lai, Z. H. Hang, H. Zheng, and C. T. Chan, “Dirac cones induced by accidental degeneracy in photonic crystals and zero-refractive-index materials,” *Nature Mater.*, vol. 10, no. 8, pp. 582–586, May 2011.
- [5] I. Liberal and N. Engheta, “Near-zero refractive index photonics,” *Nature Photon.*, vol. 11, no. 3, pp. 149–158, Mar. 2017.
- [6] A. Poddubny, I. Iorsh, P. Belov, and Y. Kivshar, “Hyperbolic metamaterials,” *Nature Photon.*, vol. 7, no. 12, pp. 948–957, Dec. 2013.
- [7] F. Wu et al., “Redshift gaps in one-dimensional photonic crystals containing hyperbolic metamaterials,” *Phys. Rev. Appl.*, vol. 10, no. 6, Dec. 2018, Art. no. 064022.
- [8] W. Zhou et al., “Progress of electromagnetic metamaterial perfect absorber based on terahertz band,” *Laser Optoelectron. Prog.*, vol. 59, no. 11, Jun. 2022, Art. no. 1100006.
- [9] S. Zong, D. Zeng, W. Yuan, G. Liu, and Z. Liu, “Recent advances on perfect light absorbers and their promise for high-performance opto-electronic devices [Invited],” *Chin. Opt. Lett.*, vol. 20, no. 7, Jul. 2022, Art. no. 073603.
- [10] N. I. Landy, S. Sajuyigbe, J. J. Mock, D. R. Smith, and W. J. Padilla, “Perfect metamaterial absorber,” *Phys. Rev. Lett.*, vol. 100, no. 20, May 2008, Art. no. 207402.
- [11] F. Ding, S. Zhong, and S. I. Bozhevolnyi, “Vanadium dioxide integrated metasurfaces with switchable functionalities at terahertz frequencies,” *Adv. Opt. Mater.*, vol. 6, no. 9, May 2018, Art. no. 1701204.
- [12] A. A. Hussain, B. Sharma, T. Barman, and A. R. Pal, “Self-powered broadband photodetector using plasmonic titanium nitride,” *ACS Appl. Mater. Interfaces*, vol. 8, no. 6, pp. 4258–4265, Feb. 2016.
- [13] Y. J. Kim et al., “Ultrathin microwave metamaterial absorber utilizing embedded resistors,” *J. Phys. D: Appl. Phys.*, vol. 50, no. 40, Oct. 2017, Art. no. 405110.
- [14] C. L. Chen et al., “Dual functional asymmetric plasmonic structures for solar water purification and pollution detection,” *Nano Energy*, vol. 51, pp. 451–456, Sep. 2018.
- [15] Y. Zhang, K. N. Zhang, T. N. Zhang, Y. Sun, X. Chen, and N. Dai, “Distinguishing plasmonic absorption modes by virtue of inverted architectures with tunable atomic-layer-deposited spacer layer,” *Nanotechnology*, vol. 25, no. 50, Dec. 2014, Art. no. 504004.
- [16] J. Chen et al., “Electrically modulating and switching infrared absorption of monolayer graphene in metamaterials,” *Carbon*, vol. 162, pp. 187–194, Jun. 2020.
- [17] H. X. Deng, L. Stan, D. A. Czaplewski, J. Gao, and X. D. Yang, “Broadband infrared absorbers with stacked double chromium ring resonators,” *Opt. Exp.*, vol. 25, no. 23, pp. 28295–28304, Nov. 2017.
- [18] M. J. Chen and Y. R. He, “Plasmonic nanostructures for broadband solar absorption based on the intrinsic absorption of metals,” *Sol. Energy Mater. Sol. Cells*, vol. 188, pp. 156–163, Dec. 2018.
- [19] O. Buchnev, N. Podoliak, T. Frank, M. Kaczmarek, L. Jiang, and V. A. Fedotov, “Controlling stiction in nano-electro-mechanical systems using liquid crystals,” *Ac Nano*, vol. 10, no. 12, pp. 11519–11524, Dec. 2016.
- [20] Y. Chen, X. Li, X. Luo, S. A. Maier, and M. Hong, “Tunable near-infrared plasmonic perfect absorber based on phase-change materials,” *Photon. Res.*, vol. 3, no. 3, pp. 54–57, Jun. 2015.
- [21] C. Liu, Y. Xu, H. Liu, M. Lin, and S. Zha, “Switchable metamaterial with terahertz buffering and absorbing performance,” *IEEE Photon. J.*, vol. 13, no. 5, Oct. 2021, Art. no. 4600408.
- [22] C. Zeng et al., “Graphene-empowered dynamic metasurfaces and metadevices,” *Opto-Electron. Adv.*, vol. 5, no. 4, May 2022, Art. no. 200098.
- [23] N. Raeis-Hosseini and J. Rho, “Dual-functional nanoscale devices using phase-change materials: A reconfigurable perfect absorber with non-volatile resistance-change memory characteristics,” *Appl. Sci.*, vol. 9, no. 3, Feb. 2019, Art. no. 564.
- [24] Y. G. Chen et al., “Hybrid phase-change plasmonic crystals for active tuning of lattice resonances,” *Opt. Exp.*, vol. 21, no. 11, pp. 13691–13698, Jun. 2013.
- [25] T. Driscoll et al., “Memory metamaterials,” *Science*, vol. 325, no. 5947, pp. 1518–1521, Sep. 2009.
- [26] S. L. Sun, Q. He, J. M. Hao, S. Y. Xiao, and L. Zhou, “Electromagnetic metasurfaces: Physics and applications,” *Adv. Opt. Photon.*, vol. 11, no. 2, pp. 380–479, Jun. 2019.
- [27] W. Zhu et al., “Controlling optical polarization conversion with  $\text{Ge}_2\text{Sb}_2\text{Te}_5$ -based phase-change dielectric metamaterials,” *Nanoscale*, vol. 10, no. 25, pp. 12054–12061, Jul. 2018.
- [28] M. J. Dicken et al., “Frequency tunable near-infrared metamaterials based on  $\text{VO}_2$  phase transition,” *Opt. Exp.*, vol. 17, no. 20, pp. 18330–18339, Sep. 2009.
- [29] Y. G. Jeong et al., “A vanadium dioxide metamaterial disengaged from insulator-to-metal transition,” *Nano Lett.*, vol. 15, no. 10, pp. 6318–6323, Oct. 2015.

- [30] H. L. Zou, Z. Y. Xiao, W. Li, and C. Li, "Double-use linear polarization convertor using hybrid metamaterial based on VO<sub>2</sub> phase transition in the terahertz region," *Appl. Phys. A*, vol. 124, no. 4, Apr. 2018, Art. no. 322.
- [31] T. C. Koethe et al., "Transfer of spectral weight and symmetry across the metal-insulator transition in VO<sub>2</sub>," *Phys. Rev. Lett.*, vol. 97, no. 11, Sep. 2006, Art. no. 116402.
- [32] K. Liu, S. Lee, S. Yang, O. Delaire, and J. Q. Wu, "Recent progresses on physics and applications of vanadium dioxide," *Mater. Today*, vol. 21, no. 8, pp. 875–896, Oct. 2018.
- [33] F. R. Hu et al., "Terahertz intensity modulator based on low current controlled vanadium dioxide composite metamaterial," *Opt. Commun.*, vol. 440, pp. 184–189, Jun. 2019.
- [34] A. Keshavarz and A. Zakery, "Ultrahigh sensitive temperature sensor based on graphene-semiconductor metamaterial," *Appl. Phys. A*, vol. 123, no. 12, Dec. 2017, Art. no. 797.
- [35] M. Wuttig and N. Yamada, "Phase-change materials for rewriteable data storage," *Nature Mater.*, vol. 6, no. 11, pp. 824–832, Nov. 2007.
- [36] S. Yang, M. Vaseem, and A. Shamim, "Fully inkjet-printed VO<sub>2</sub>-based radio-frequency switches for flexible reconfigurable components," *Adv. Mater. Technol.*, vol. 4, no. 1, Jan. 2019, Art. no. 1800276.
- [37] Y. Ren, T. Zhou, C. Jiang, and B. Tang, "Thermally switching between perfect absorber and asymmetric transmission in vanadium dioxide-assisted metamaterials," *Opt. Exp.*, vol. 29, no. 5, pp. 7666–7679, Mar. 2021.
- [38] Z. Y. Song, A. Chen, and J. H. Zhang, "Terahertz switching between broadband absorption and narrowband absorption," *Opt. Exp.*, vol. 28, no. 2, pp. 2037–2044, Jan. 2020.
- [39] Z. Song and J. Zhang, "Achieving broadband absorption and polarization conversion with a vanadium dioxide metasurface in the same terahertz frequencies," *Opt. Exp.*, vol. 28, no. 8, pp. 12487–12497, Apr. 2020.
- [40] E. D. Palik, *Handbook of Optical Constants of Solids II*. Boston, MA, USA: Academic, 1991.
- [41] F. Fan, Y. Hou, Z. W. Jiang, X. H. Wang, and S. J. Chang, "Terahertz modulator based on insulator-metal transition in photonic crystal waveguide," *Appl. Opt.*, vol. 51, no. 20, pp. 4589–4596, Jul. 2012.
- [42] L. Cai, Z. Zhang, H. Xiao, S. Chen, and J. Fu, "An eco-friendly imprinted polymer based on graphene quantum dots for fluorescent detection of p-nitroaniline," *RSC Adv.*, vol. 9, no. 71, pp. 41383–41391, Dec. 2019.
- [43] L. Fang, H. Z. Zhao, J. Wang, Y. Liang, P. P. Lu, and Z. X. Yang, "Magnetic graphene modified imprinted electrochemical sensor for detection of 4-Octylphenol," *Chin. J. Anal. Chem.*, vol. 44, no. 6, pp. 908–914, Jun. 2016.
- [44] J. H. Li et al., "Facile synthesis of Ag@Cu<sub>2</sub>O heterogeneous nanocrystals decorated N-doped reduced graphene oxide with enhanced electrocatalytic activity for ultrasensitive detection of H<sub>2</sub>O<sub>2</sub>," *Sens. Actuators, B*, vol. 260, pp. 529–540, May 2018.
- [45] Y. H. Liu, M. L. Bo, X. X. Yang, P. P. Zhang, C. Q. Sun, and Y. L. Huang, "Size modulation electronic and optical properties of phosphorene nanoribbons: DFT-BOLS approximation," *Phys. Chem. Chem. Phys.*, vol. 19, no. 7, pp. 5304–5309, Feb. 2017.
- [46] S. Quader, M. R. Akram, F. Xiao, and W. Zhu, "Graphene based ultra-broadband terahertz metamaterial absorber with dual-band tunability," *J. Opt.*, vol. 22, no. 9, Sep. 2020, Art. no. 095104.
- [47] M. R. Akram, M. Q. Mehmood, X. D. Bai, R. H. Jin, M. Premaratne, and W. R. Zhu, "High efficiency ultrathin transmissive metasurfaces," *Adv. Opt. Mater.*, vol. 7, no. 11, Jun. 2019, Art. no. 1801628.
- [48] J. K. Li et al., "Broadband solar energy absorber based on monolayer molybdenum disulfide using tungsten elliptical arrays," *Mater. Today Energy*, vol. 16, Jun. 2020, Art. no. 100390.
- [49] J. Ordonez-Miranda, Y. Ezzahri, K. Joulain, J. Drevillon, and J. J. Alvarado-Gil, "Modeling of the electrical conductivity, thermal conductivity, and specific heat capacity of VO<sub>2</sub>," *Phys. Rev. B*, vol. 98, no. 7, Aug. 2018, Art. no. 075144.